PHYSICAL REVIEW C VOLUME 58, NUMBER 3 SEPTEMBER 1998

Charge asymmetry of the nucleon-nucleon interaction

G. Q. Li* and R. Machleidt†
Department of Physics, University of Idaho, Moscow, Idaho 83844
(Received 7 April 1998)

Based upon the Bonn meson-exchange model for the nucleon-nucleon (NN) interaction, we study systematically the charge-symmetry-breaking (CSB) of the NN interaction due to nucleon mass splitting. Particular attention is paid to CSB generated by the 2π-exchange contribution to the NN interaction, $\pi\rho$ diagrams, and other multimeson exchanges. We calculate the CSB differences in the $^1S_0$ effective range parameters as well as phase shift differences in S, P, and higher partial waves up to 300 MeV laboratory energy. We find a total CSB difference in the singlet scattering length of 1.6 fm which explains the empirical value accurately. The corresponding CSB phase-shift differences are appreciable at low energy in the $^1S_0$ state. In the other partial waves, the CSB splitting of the phase shifts is small and increases with energy, with typical values in the order of 0.1° at 300 MeV in P and D waves. [S0556-2813(98)05609-X]

PACS number(s): 24.80.+y, 11.30.Hv, 13.75.Cs, 21.30.Cb

I. INTRODUCTION

Charge symmetry is the equality of proton-proton (pp) and neutron-neutron (nn) forces—after electromagnetic effects are removed. This symmetry, which is slightly broken, has long been a subject of research in nuclear physics (for reviews see, e.g., Refs. [1–4]). Traditionally, empirical information on the charge asymmetry of the nuclear force comes mainly from few-body systems. The nucleon-nucleon (NN) scattering length in the $^1S_0$ state plays a special role. As there exists an almost bound state in that partial wave, the (negative) scattering length is extremely sensitive to small differences in the strength of the force. The pp effective range parameters (scattering length a and effective range r) are obtained with very high precision from low-energy pp cross section data. However, since we are interested here in the strong force, electromagnetic effects have to be removed, which introduces model dependence. Using several realistic NN potential models, the pure strong-interaction pp effective range parameters are determined to be [2]

$$a^N_{pp} = -17.3 \pm 0.4 \text{ fm}, \tag{1}$$

$$r^N_{pp} = 2.85 \pm 0.04 \text{ fm}, \tag{2}$$

where the errors state the uncertainty due to model dependence.

Since nn scattering experiments are not yet feasible, the nn effective range parameters are not measured directly; they are extracted from few-body reactions, mainly $D(n,nn)p$ and $D(\pi^-,\gamma)2n$. Recent measurements of these reactions and their analysis have resulted in the following recommended values [1,2]:

$$a^N_{nn} = -18.8 \pm 0.3 \text{ fm}, \tag{3}$$

$$r^N_{nn} = 2.75 \pm 0.11 \text{ fm}. \tag{4}$$

It is thus evident that in the $^1S_0$ state, the nn strong interaction is slightly more attractive than the pp one. From the above semiempirical values, we see that charge symmetry is broken by the following amounts:

$$\Delta a_{CSB} \equiv a^N_{pp} - a^N_{nn} = 1.5 \pm 0.5 \text{ fm}, \tag{5}$$

$$\Delta r_{CSB} \equiv r^N_{pp} - r^N_{nn} = 0.10 \pm 0.12 \text{ fm}. \tag{6}$$

Information about charge symmetry breaking (CSB) can also be inferred from the binding energy differences of so-called mirror nuclei. The most studied case is the ^{3}He-^{3}H mirror pair. Experimentally it was found that ^{3}H is more deeply bound than ^{3}He by 764 keV. Model-independent calculations of the Coulomb energy difference and other subtle electromagnetic effects yield a binding energy difference of about 683 ± 29 keV [5]. It has been shown that the remaining discrepancy can be explained by a charge-symmetry-breaking nuclear force that is consistent with the empirical asymmetry in the singlet scattering length [6].

According to our current understanding, CSB is due to a mass difference between the up and down quark and electromagnetic interactions. On the hadronic level, this has various consequences: mixing of mesons of different isospin but same spin and parity, and mass differences between hadrons of the same isospin multiplet.

The difference between the masses of neutron and proton represents the most basic cause for CSB. Therefore, it is important to have a very thorough accounting of this effect. This is the subject of the present paper.

The $n-p$ mass difference, which is well known to be 1.2933 MeV [9], affects the kinetic energy of the nucleons. Besides this, it has also an impact on all meson-exchange diagrams that contribute to the nuclear force.

In Sec. II, we will briefly outline the formalism of the Bonn model for the NN interaction that this study is based upon. In Sec. III, we will go—step by step—through the various meson-exchange contributions to the nuclear force and calculate for each step the CSB effect due to nucleon

*Present address: Department of Physics, SUNY, Stony Brook, NY 11794.
†Electronic address: machleid@uidaho.edu

mass splitting. In particular, we will present the effect on the singlet effective range parameters and on phase shifts of NN scattering up to 300 MeV laboratory energy and up to orbital angular momentum $L=2$. Section IV concludes the paper.

II. SKETCH OF THE MODEL

We base our investigation on the comprehensive Bonn full model for the NN interaction. This model has been described in length in the literature [4,7,8]. Therefore, we will summarize here only those facts which are important for the issue under consideration.

The Bonn model uses an effective, field-theoretic approach, in which the interaction between two nucleons is created solely from the exchange of mesons, namely, π, $\rho(770)$, $\omega(782)$, $a_0/\delta(980)$, and $\sigma'(550)$. Besides the nucleon, the $\Delta(1232)$ isobar is also taken into account. In its original version [7], the Bonn model used averages for baryon and meson masses and, thus, was charge independent; it was fitted to the neutron-proton data. In this paper, these subtleties will be treated accurately.

The interaction Lagrangians involving pions are

$$\mathcal{L}_{\pi NN}=\frac{f_{\pi NN}}{m_{\pi^\pm}}\bar{\psi}\gamma_\mu\gamma_5\boldsymbol{\tau}\psi\cdot\partial^\mu\boldsymbol{\varphi}_\pi, \tag{7}$$

$$\mathcal{L}_{\pi N\Delta}=\frac{f_{\pi N\Delta}}{m_{\pi^\pm}}\bar{\psi}\boldsymbol{T}\psi_\mu\cdot\partial^\mu\boldsymbol{\varphi}_\pi+\text{H.c.}, \tag{8}$$

with ψ the nucleon, ψ_μ the Δ (Rarita-Schwinger spinor), and $\boldsymbol{\varphi}_\pi$ the pion fields. τ are the usual Pauli matrices describing isospin 1/2 and $\boldsymbol{T}$ is the isospin transition operator. H.c. denotes the Hermitian conjugate.

The above Lagrangians are divided by $m_{\pi^\pm}$ to make the coupling constants f dimensionless. Following established conventions [10], we always use $m_{\pi^\pm}$ as the scaling mass. It may be tempting to use m_{π^0} for π^0 coupling. Notice, however, that the scaling mass could be anything. Therefore, it is reasonable to keep the scaling mass constant within SU(3) multiplets [10]. This avoids the creation of unmotivated charge dependence.

It is important to stress that—as evidenced by the above πNN Langrangian—we use the pseudovector (pv) or gradient coupling for the pion. Alternatively, on can also use the pseudoscalar (ps) coupling,

$$\mathcal{L}^{(\mathrm{ps})}_{\pi NN}=g_{\pi NN}\bar{\psi}i\gamma_5\boldsymbol{\tau}\psi\cdot\boldsymbol{\varphi}_\pi. \tag{9}$$

For an on-shell process, the two couplings yield the same if the coupling constants are related by

$$g_{\pi NN}=\left(\frac{M_1+M_2}{m_{\pi^\pm}}\right)f_{\pi NN}, \tag{10}$$

with M_1 and M_2 the masses of the two nucleons involved. This relationship is charge dependent due to the two nucleon masses. As a consequence, CSB effects will come out (noticeably) different depending on if the ps or the pv coupling is used. Nonlinear realizations of chiral symmetry, which are currently fashionable, prefer the pv coupling over the ps coupling. Following this trend, we use the pv coupling.

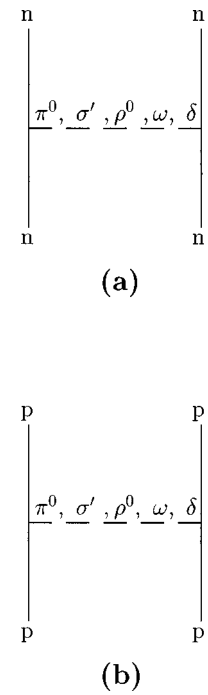

FIG. 1. One-boson-exchange (OBE) contributions to (a) nn and (b) pp scattering.

The couplings of ρ mesons to nucleons and Δ isobars are described by the Lagrangians

$$\mathcal{L}_{\rho NN}=g_{\rho NN}\bar{\psi}\gamma_\mu\boldsymbol{\tau}\psi\cdot\boldsymbol{\varphi}^\mu_\rho+\frac{f_{\rho NN}}{4M_p}\bar{\psi}\sigma_{\mu\nu}\boldsymbol{\tau}\psi\cdot(\partial^\mu\boldsymbol{\varphi}^\nu_\rho-\partial^\nu\boldsymbol{\varphi}^\mu_\rho), \tag{11}$$

$$\mathcal{L}_{\rho N\Delta}=i\frac{f_{\rho N\Delta}}{m_{\rho^\pm}}\bar{\psi}\gamma_5\gamma_\mu\boldsymbol{T}\psi_\nu\cdot(\partial^\mu\boldsymbol{\varphi}^\nu_\rho-\partial^\nu\boldsymbol{\varphi}^\mu_\rho)+\text{H.c.} \tag{12}$$

We have to draw attention to the fact that—no matter to which nucleon the ρ couples—in the second part of the ρNN Langrangian, we always use the proton mass M_p as the scaling mass. With this, we follow established conventions, as discussed above in conjunction with the pion Langrangians. We note that disregarding this point would generate noticeable, but unmotivated CSB.

Finally, the Lagrangians for ω and σ' are

$$\mathcal{L}_{\omega NN}=g_{\omega NN}\bar{\psi}\gamma_\mu\psi\varphi^\mu_\omega, \tag{13}$$

$$\mathcal{L}_{\sigma' NN}=g_{\sigma' NN}\bar{\psi}\psi\varphi_{\sigma'}. \tag{14}$$

Starting from these Lagrangians, irreducible diagrams up to fourth order are evaluated using old-fashioned and time-ordered perturbation theory. Some important diagrams (but not all) are shown in Figs. 1–4. The sum of all irreducible diagrams included in the model is, by definition, the quasipotential V. Mathematically, this quasipotential is the kernel of the scattering equation. For an uncoupled partial wave with angular momentum J, this equation reads

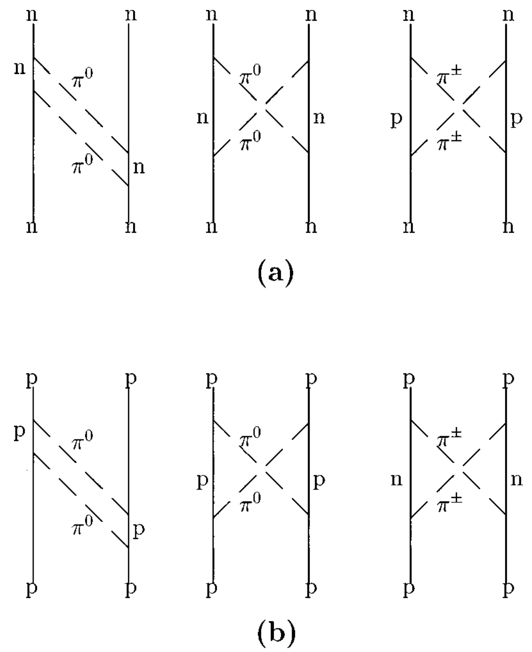

FIG. 2. Irreducible 2π-exchange diagrams with NN intermediate states for (a) nn and (b) pp scattering.

$$R_J(q',q)=V_J(q',q)+\mathcal{P}\int_0^\infty \frac{dkk^2}{2E_q-2E_k}V_J(q',k)R_J(k,q), \tag{15}$$

with q, k, and q' the magnitude of the relative momenta of the two interacting nucleons in the initial, intermediate, and final states, respectively; $E_q=\sqrt{M^2+q^2}$ and $E_k=\sqrt{M^2+k^2}$ with M the correct mass of the nucleon involved in the scattering process under consideration. The principal value is denoted by $\mathcal{P}$, and R is commonly called the K matrix. By solving this equation, the kernel or quasipotential is iterated infinitely many times. This is equivalent to solving the Schrödinger equation.

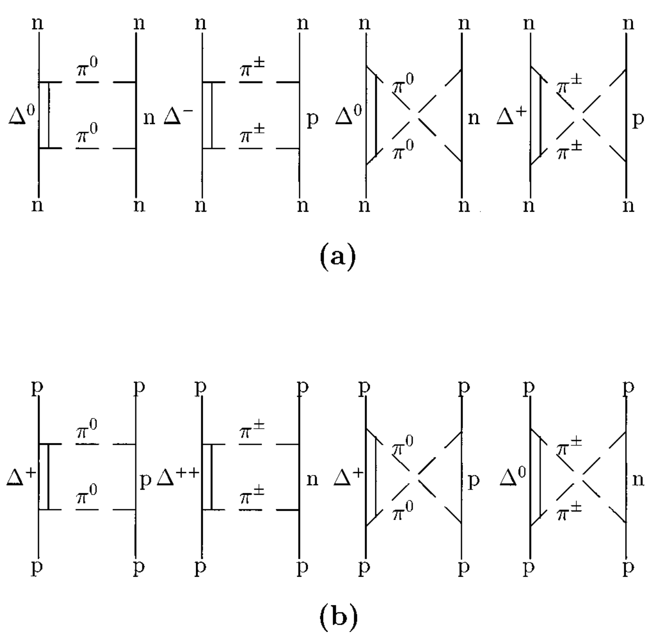

FIG. 3. 2π-exchange contributions with $N\Delta$ intermediate states to (a) nn and (b) pp scattering.

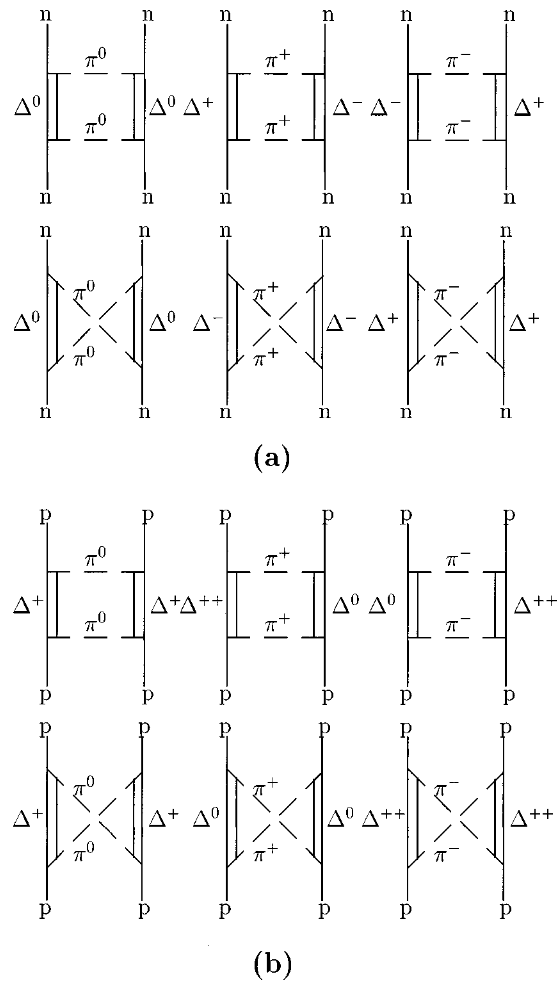

FIG. 4. 2π-exchange contributions with $\Delta\Delta$ intermediate states to (a) nn and (b) pp scattering.

From the on-shell R matrix, phase shifts for uncoupled partial waves are obtained through

$$\tan\,\delta_J(T_{\rm lab})=-\frac{\pi}{2}qE_qR_J(q,q), \tag{16}$$

where q denotes the on-shell momentum in the center-of-mass system of the two nucleons which is related to the laboratory kinetic energy by $T_{\rm lab}=2q^2/M$.

Further details concerning the formalism can be found in Appendixes A–C of Ref. [7].

III. CSB DUE TO THE NUCLEON MASS DIFFERENCE

It is the purpose of the present investigation to take the nucleon mass splitting accurately into account, which leads to CSB. Therefore, we use exact values for the proton mass M_p and neutron mass M_n [9]:

$$M_p=938.2723\ \text{MeV}, \tag{17}$$

$$M_n=939.5656\ \text{MeV}. \tag{18}$$

We start with pp scattering for which the one-boson-exchange contribution is depicted in Fig. 1(b) and 2π-exchange contributions are shown in Figs. 2(b), 3(b), and

TABLE I. CSB differences of the $^1S_0$ effective range parameters as explained in the text. 2π denotes the sum of all 2π contributions and $\pi\rho$ the sum of all $\pi\rho$ contributions. TBE (noniterative two-boson exchange) is the sum of 2π, $\pi\rho$, and $(\pi\sigma+\pi\omega)$.

	Kin. en.	OBE	2π	$\pi\rho$	$\pi\sigma+\pi\omega$	TBE	Total
$\Delta a_{\rm CSB}$ (fm)	0.246	0.013	2.888	–1.537	–0.034	1.316	1.575
$\Delta r_{\rm CSB}$ (fm)	0.004	0.001	0.055	–0.031	–0.001	0.023	0.027

4(b). Note that in all of these diagrams, the proton carries the exact proton mass M_p and the neutron, which occurs in some intermediate states, carries the exact neutron mass M_n. For the Δ isobars, which are excited in some intermediate states in Figs. 3 and 4, the average mass $M_\Delta=1232$ MeV is used.

For the pp case, our model yields -17.20 fm for the singlet scattering length and 2.88 fm for the corresponding effective range, consistent with Eqs. (1) and (2).

Switching now—step by step—from pp to nn scattering will change the effective range parameters and the phase shifts, in violation of charge symmetry.

The differences that occur for the effective range parameters are given in Tables I and II. Note that the relationship between the CSB potential and the corresponding change of the scattering length, $\Delta a_{\rm CSB}$, is highly nonlinear. As discussed in Refs. [11,12], when the scattering length changes from a_1 to a_2 due to a CSB potential $\Delta V=V_1-V_2$, the relationship is

$$\frac{1}{a_2}-\frac{1}{a_1}=M_N\int_0^\infty \Delta V u_1 u_2 dr \tag{19}$$

or

$$a_1-a_2=a_1a_2M_N\int_0^\infty \Delta V u_1 u_2 dr, \tag{20}$$

with u_1 and u_2 the zero-energy $^1S_0$ wave functions normalized such that $u(r\to\infty)\to(1-r/a)$. Thus, the perturbation expansion concerns the inverse scattering length. As clearly evident from Eq. (20), the change of the scattering length depends on the ''starting value'' a_1 to which the effect is added. In our calculations, CSB effects are generated step by step, which implies that the starting value a_1 is different for different CSB effects. This distorts the relative size of the scattering length differences. To make the relative comparison meaningful, we have rescaled our results for $\Delta a_{\rm CSB}$ according to a prescription given by Ericson and Miller [11], which goes as follows. Assume that the ''starting value'' for the scattering length is a_1 and a certain CSB effect brings it up to a_2. Then, the resulting scattering length difference (a_1-a_2) is rescaled by

$$\Delta a=(a_1-a_2)\frac{a_{pp}a_{nn}}{a_1a_2}, \tag{21}$$

with $a_{pp}=-17.3$ fm and $a_{nn}=-18.8$ fm. This will make Δa independent of the choice for a_1. The numbers given in Tables I and II for $\Delta a_{\rm CSB}$ are all rescaled according to this prescription.

To state the effects of CSB on the NN phase shifts, we introduce for each LSJ state the CSB phase shift difference $\Delta\delta^{LSJ}_{\rm CSB}(T_{\rm lab})$, defined by

$$\Delta\delta^{LSJ}_{\rm CSB}(T_{\rm lab})\equiv\delta^{LSJ}_{nn}(T_{\rm lab})-\delta^{LSJ}_{pp}(T_{\rm lab}), \tag{22}$$

where δ^{LSJ}_{nn} denotes the nn and δ^{LSJ}_{pp} the pp phase shifts (without electromagnetic effects), respectively.

The irreducible diagrams included in the quasipotential or kernel can be subdivided into several groups. After discussing the effect from the kinetic energy, we will describe each group of diagrams and the implications for CSB.

(1) *Kinetic energy* (column ''Kin. en.'' in Tables I and III). The kinetic energy is smaller for the neutron because of its larger mass. This reduces the magnitude of the energy denominator in Eq. (15) for nn scattering as compared to pp, thus enhancing the (attractive) integral term for nn. In addition, the factor E_q in Eq. (16) is larger for the larger nucleon mass, which results in an overall enhancement of the magnitude of the nn phase shifts. The combined effect yields larger nn phase shifts as compared to pp if the nuclear potential is attractive and vice versa if the nuclear potential is repulsive. This can be understood more easily in the framework of the radial Schrödinger equation in which the effective potential is MV. Thus, no matter if the nuclear potential V is attractive or repulsive, its effect on the phase shifts is always enhanced for the larger nucleon mass M. This explains why in $^3P_1$ the CSB phase shift splitting, Eq. (22), comes out negative (repulsive potential, negative phase shift), while it is positive in all other partial waves listed in Table III (column ''Kin. en.'') where the potentials are attractive (positive phase shifts). The magnitude of the singlet scattering length increases by 0.25 fm (cf. Table I, column ''Kin. en.'') for nn scattering as compared to pp. This is, of course, well known, and the effect on the scattering length is

TABLE II. CSB differences of the $^1S_0$ effective range parameters from 2π and $\pi\rho$ diagrams as explained in the text.

	$2\pi NN$	$2\pi N\Delta$	$2\pi\Delta\Delta$	$\pi\rho NN$	$\pi\rho N\Delta$	$\pi\rho\Delta\Delta$	Sum
$\Delta a_{\rm CSB}$ (fm)	0.374	1.852	0.662	–0.484	–1.184	0.130	1.350
$\Delta r_{\rm CSB}$ (fm)	0.005	0.036	0.014	–0.010	–0.025	0.003	0.024

TABLE III. CSB phase shift differences (in degrees) as defined in Eq. (22). Notation as in Table I.

$T_{\rm lab}$ (MeV)	Kin. en.	OBE	2π	$\pi\rho$	$\pi\sigma+\pi\omega$	TBE	Total
			$^1S_0$				
1	0.287	0.015	3.417	-1.856	-0.041	1.520	1.822
5	0.162	0.010	1.850	-1.007	-0.022	0.810	0.982
10	0.104	0.006	1.409	-0.773	-0.018	0.618	0.727
25	0.066	0.004	0.995	-0.585	-0.014	0.396	0.466
50	0.053	0.003	0.778	-0.460	-0.011	0.291	0.347
100	0.036	0.004	0.585	-0.378	-0.008	0.199	0.239
150	0.019	0.006	0.567	-0.387	-0.006	0.174	0.198
200	0.015	0.021	0.565	-0.407	-0.004	0.154	0.190
300	0.005	0.029	0.562	-0.446	-0.001	0.116	0.149
			$^3P_0$				
5	0.004	0.003	0.001	0.000	0.000	0.001	0.009
10	0.010	0.006	0.001	0.001	0.000	0.002	0.019
25	0.020	0.014	0.003	0.003	0.001	0.007	0.042
50	0.025	0.018	0.006	0.006	0.002	0.014	0.057
100	0.025	0.014	0.008	0.010	0.003	0.021	0.060
150	0.016	0.017	0.007	0.012	0.004	0.023	0.057
200	0.008	0.022	0.006	0.014	0.005	0.024	0.054
300	0.004	0.023	0.002	0.016	0.005	0.022	0.050
			$^3P_1$				
5	-0.002	-0.001	0.002	-0.001	0.000	0.001	-0.002
10	-0.004	-0.001	0.006	-0.002	0.000	0.004	-0.002
25	-0.011	0.001	0.017	-0.006	0.000	0.011	0.000
50	-0.017	0.002	0.044	-0.019	0.000	0.025	0.010
100	-0.025	0.008	0.092	-0.046	0.000	0.045	0.028
150	-0.033	0.016	0.139	-0.081	0.000	0.058	0.041
200	-0.041	0.023	0.185	-0.112	0.001	0.074	0.056
300	-0.059	0.033	0.278	-0.195	0.001	0.084	0.058
			$^1D_2$				
25	0.001	0.001	0.002	0.000	0.000	0.002	0.004
50	0.004	0.001	0.008	-0.001	0.000	0.007	0.012
100	0.007	0.002	0.031	-0.007	0.000	0.024	0.033
150	0.011	0.003	0.061	-0.018	0.000	0.043	0.057
200	0.012	0.003	0.095	-0.034	0.000	0.061	0.076
300	0.014	0.003	0.178	-0.078	0.000	0.100	0.117
			$^3P_2$				
5	0.001	0.000	0.002	0.000	0.000	0.002	0.003
10	0.002	0.001	0.006	-0.001	0.000	0.005	0.007
25	0.005	0.002	0.023	-0.006	0.000	0.018	0.025
50	0.014	0.002	0.054	-0.015	0.000	0.040	0.056
100	0.023	0.001	0.114	-0.036	0.001	0.079	0.102
150	0.026	0.001	0.154	-0.055	0.002	0.101	0.128
200	0.025	0.000	0.177	-0.068	0.003	0.112	0.137
300	0.023	0.000	0.237	-0.095	0.003	0.144	0.167

usually quoted to be 0.30 fm [13]. Our value is slightly smaller which can be attributed to the use of relativistic kinetic energies in our model.

(2) *One-boson-exchange* (OBE), Fig. 1, contributions mediated by $\pi^0(135)$, $\rho^0(770)$, $\omega(782)$, $a_0/\delta(980)$, and $\sigma'(550)$. In the Bonn model [7], the σ' describes only the correlated 2π exchange in $\pi\pi$ S waves (and not the uncorrelate 2π exchange since the latter is calculated explicitly; cf. Figs. 2–4). Charge symmetry is broken by the fact that for pp scattering the proton mass is used in the Dirac spinors representing the four external legs [Fig. 1(b)], while for nn scattering the neutron mass is applied [Fig. 1(a)]. The CSB effect from the OBE diagrams is extremely small (cf. Tables I and III, column ''OBE'').

(3) 2π *exchange with NN intermediate states* ($2\pi NN$), Fig. 2. Notice first that only noniterative diagrams are to be

considered, since the iterative ones are generated by the scattering equation (15) from the OBE diagrams. In our calculations, we include always all time orderings (except those with antibaryons in intermediate states); to save space, we display, however, only a few characteristic graphs in Fig. 2 (this is also true for all diagrams shown or discussed below). Part (a) of Fig. 2 applies to nn scattering, while part (b) refers to pp scattering. Notice that when charged-pion exchange is involved, the intermediate-state nucleon differs from that of the external legs. This is an important subtlety that we account for accurately in our calculations; neglecting this effect causes a systematic error of the order of 100%. Numerical results for this class of diagrams are given in Tables II and IV, column ''$2\pi NN$.''

(4) *2π exchange with* N Δ *intermediate states* ($2\pi N\Delta$), Fig. 3. This class of diagrams causes by far the largest CSB effect on the scattering length (Table II) as well as on the phase shifts (Table IV). Again, it is important in all of these diagrams to take the intermediate-state nucleon mass correctly into account.

(5) *2π exchange with $\Delta\Delta$ intermediate states* ($2\pi\Delta\Delta$), Fig. 4. The effects are smaller than for $2\pi N\Delta$ because there are no nucleon intermediate states. Thus, the nucleon mass splitting affects only the outer legs which typically results in a small effect.

(6) *$\pi\rho$ exchange with NN intermediate states* ($\pi\rho NN$). Graphically, the $\pi\rho NN$ diagrams can be obtained by replacing, in each diagram of Fig. 2, one pion by a ρ meson of the same charge state (because of this simple analogy, we do not show the $\pi\rho$ diagrams explicitly here). In our calculations, the CSB effects of the $\pi\rho$ diagrams with NN intermediate states are taken into account accurately. The effect is typically opposite to the one from $2\pi NN$ exchange.

(7) *$\pi\rho$ exchange with* N Δ *intermediate states* ($\pi\rho N\Delta$). Concerning the $\pi\rho$ diagrams with Δ intermediate states a comment is in place. In the Bonn model [7], the crossed $\pi\rho$ diagrams with Δ intermediate states are included in terms of an approximation. It is assumed that they differ from the corresponding box diagrams [i.e., the diagrams on the left-hand side of Fig. 3 and the ones in the first row of Figs. 4(a) and 4(b), but with one π replaced by one ρ] only by the isospin factor. Thus, the $\pi\rho$ box diagrams with Δ intermediate states are multiplied by an isospin factor that is equal to the sum of the isospin factors for box and crossed box. The $\pi\rho N\Delta$ effect is in general substantial and typically of the opposite sign as compared to $2\pi N\Delta$.

(8) *$\pi\rho$ exchange with $\Delta\Delta$ intermediate states* ($\pi\rho\Delta\Delta$). The effects are very small.

(9) *Further 3π and 4π contributions* ($\pi\sigma+\pi\omega$). The Bonn potential also includes some 3π exchanges that can be approximated in terms of $\pi\sigma$ diagrams and 4π exchanges of $\pi\omega$ type. The sum of these contributions is small. These diagrams have NN intermediate states (similar to Fig. 2, but with one of the two exchanged pions replaced by an isospin-zero boson) and, thus, are of intermediate range. Except for $^1S_0$, their effect is negligible.

This finishes our detailed presentation of the relevant diagrams and their CSB effects which are plotted in Figs. 5 and 6. The total CSB splitting of the singlet scattering length amounts to 1.58 fm (cf. last column of Table I) which agrees well with the empirical value 1.5 ± 0.5 fm, Eq. (5). The sum of all CSB effects on phase shifts is given in the last column of Table III and plotted by the solid curve in Fig. 5. The largest total effect listed in Table III is 1.8° in $^1S_0$ at 1 MeV. In the S wave, the effect decreases with energy and is 0.15° at 300 MeV. In P and D waves the CSB effect on phase shifts increases with energy and is typically in the order of 0.1° at 300 MeV. We do not list our results for partial waves with $L\geqslant 3$, since the CSB effect becomes negligibly small for high L: less than 0.02° at 300 MeV and 0.01° or less at 200 MeV for F and G waves and even smaller for higher partial waves.

Since the pion is involved in almost all diagrams considered in this study, the CSB effect depends on the πNN coupling constant. In the present calculations, we follow the Bonn model [7]: we assume charge independence of the coupling constant and use $f^2_{\pi NN}/4\pi=0.0795$ which, via Eq. (10), translates into $g^2_{\pi NN}/4\pi=14.4$. In recent years, there has been some controversy about the precise value of the πNN coupling constant. Unfortunately, the problem is far from being settled. Based upon NN phase-shift analysis, the Nijmegen group [14] advocates the ''small'' charge-independent value $g^2_\pi/4\pi=13.5(1)$, while a very recent determination by the Uppsala group [15] based upon high-precision np charge-exchange data at 162 MeV seems to confirm the large ''textbook'' value $g^2_{\pi^\pm}/4\pi=14.5(3)$. Other recent determinations are in between the two extremes: The VPI group [16] quotes $g^2_\pi/4\pi=13.77(15)$ from πN and NN analysis with no evidence for charge dependence. Bugg and Machleidt [17] obtain $g^2_{\pi^\pm}/4\pi=13.69(39)$ and $g^2_{\pi^0}/4\pi=13.94(24)$ from the analysis of NN elastic data between 210 and 800 MeV. Because of this large uncertainty in the πNN coupling constant, it is of interest to know how the CSB effects depend on this constant. Naturally, the 2π contributions are proportional to g^4_π [18] and the $\pi\rho$ ones to g^2_π. Since the two contributions carry (in general) opposite signs and vary in their relative magnitude from partial wave to partial wave, there is no simple rule for how the total CSB effect depends on g_π. The value $g^2_\pi/4\pi=13.6$ is currently fashionable among the new generation of high-precision NN potentials [19–21]. For that reason, we have repeated our CSB calculations using $g^2_\pi/4\pi=13.6$ and find that the total $\Delta a_{\rm CSB}$ is reduced by about 15% as compared to the calculation using $g^2_\pi/4\pi=14.4$ (Table I). The phase-shift differences are reduced by roughly the same percentage in most partial waves. The exact numbers for $g^2_\pi/4\pi=13.6$ will be published elsewhere.

IV. SUMMARY AND CONCLUSIONS

Based upon the Bonn meson-exchange model for the NN interaction, we have calculated the CSB effects due to nucleon mass splitting on the phase shifts of NN scattering and the singlet effective range parameters. We give results for partial waves up to $L=2$ and laboratory energies below 300 MeV.

A remarkable finding is that the experimental CSB difference in the singlet scattering length can be explained from nucleon mass splitting alone.

Concerning phase shift differences, we find the largest in the $^1S_0$ state where they are most noticeable at low energy;

TABLE IV. CSB phase shift differences (in degrees) as defined in Eq. (22) from the various 2π and $\pi\rho$-exchange contributions as defined in the text.

T_{lab} (MeV)	$2\pi NN$	$2\pi N\Delta$	$2\pi\Delta\Delta$	$\pi\rho NN$	$\pi\rho N\Delta$	$\pi\rho\Delta\Delta$	Sum
			$^1S_0$				
1	0.424	2.184	0.808	-0.592	-1.418	0.154	1.561
5	0.224	1.190	0.436	-0.317	-0.776	0.086	0.843
10	0.164	0.909	0.336	-0.242	-0.597	0.067	0.636
25	0.099	0.648	0.248	-0.182	-0.452	0.049	0.410
50	0.059	0.514	0.204	-0.138	-0.366	0.044	0.318
100	0.012	0.406	0.168	-0.105	-0.317	0.044	0.207
150	-0.005	0.392	0.180	-0.106	-0.331	0.049	0.180
200	-0.020	0.395	0.190	-0.108	-0.360	0.061	0.158
300	-0.065	0.405	0.223	-0.113	-0.413	0.080	0.117
			$^3P_0$				
5	-0.001	0.001	0.000	0.000	0.000	0.000	0.001
10	-0.003	0.004	0.001	0.000	0.001	0.000	0.002
25	-0.012	0.013	0.002	0.000	0.003	-0.001	0.006
50	-0.022	0.024	0.004	0.001	0.006	-0.001	0.012
100	-0.036	0.038	0.006	0.001	0.011	-0.002	0.018
150	-0.044	0.044	0.007	0.000	0.014	-0.003	0.019
200	-0.051	0.049	0.008	0.000	0.017	-0.003	0.019
300	-0.064	0.057	0.009	-0.003	0.022	-0.004	0.017
			$^3P_1$				
5	0.001	0.001	0.000	0.000	0.000	0.000	0.001
10	0.002	0.003	0.000	-0.001	-0.001	0.000	0.004
25	0.006	0.011	0.001	-0.002	-0.004	0.000	0.011
50	0.013	0.029	0.002	-0.006	-0.013	0.000	0.025
100	0.024	0.063	0.005	-0.014	-0.032	0.000	0.046
150	0.032	0.100	0.007	-0.024	-0.056	-0.001	0.059
200	0.038	0.139	0.009	-0.036	-0.074	-0.002	0.073
300	0.050	0.217	0.011	-0.051	-0.143	-0.001	0.083
			$^1D_2$				
25	0.001	0.001	0.000	0.000	0.000	0.000	0.002
50	0.003	0.005	0.000	0.000	-0.001	0.000	0.007
100	0.010	0.019	0.002	-0.002	-0.005	0.000	0.024
150	0.016	0.041	0.003	-0.004	-0.013	0.000	0.043
200	0.021	0.071	0.004	-0.005	-0.029	0.000	0.061
300	0.027	0.142	0.009	-0.011	-0.065	-0.001	0.100
			$^3P_2$				
5	0.000	0.001	0.000	0.000	0.000	0.000	0.002
10	0.001	0.004	0.001	0.000	-0.001	0.000	0.005
25	0.003	0.015	0.006	-0.002	-0.003	-0.001	0.018
50	0.005	0.035	0.014	-0.005	-0.007	-0.003	0.039
100	0.006	0.075	0.033	-0.013	-0.016	-0.007	0.078
150	0.005	0.102	0.047	-0.019	-0.025	-0.011	0.099
200	0.003	0.120	0.054	-0.022	-0.032	-0.014	0.109
300	-0.001	0.155	0.083	-0.031	-0.044	-0.021	0.142

e.g., at 1 MeV, the difference is 1.8°, indicating that the *nn* nuclear force is more attractive than the *pp* one. The $^1S_0$ phase-shift difference decreases with increasing energy and is about 0.15° at 300 MeV.

The CSB effect on the phase shifts of higher partial waves is small; in *P* and *D* waves, typically of the order of 0.1° at 300 MeV and less at lower energies. This is substantially smaller than what is required phenomenologically to solve the so-called A_y puzzle in elastic nucleon-deuteron scattering at low energies [22].

The major part of the CSB effect comes from diagrams of 2π exchange where those with $N\Delta$ intermediate states make the largest contribution. We also study the CSB effect from irreducible diagrams that exchange a π and ρ meson. To our

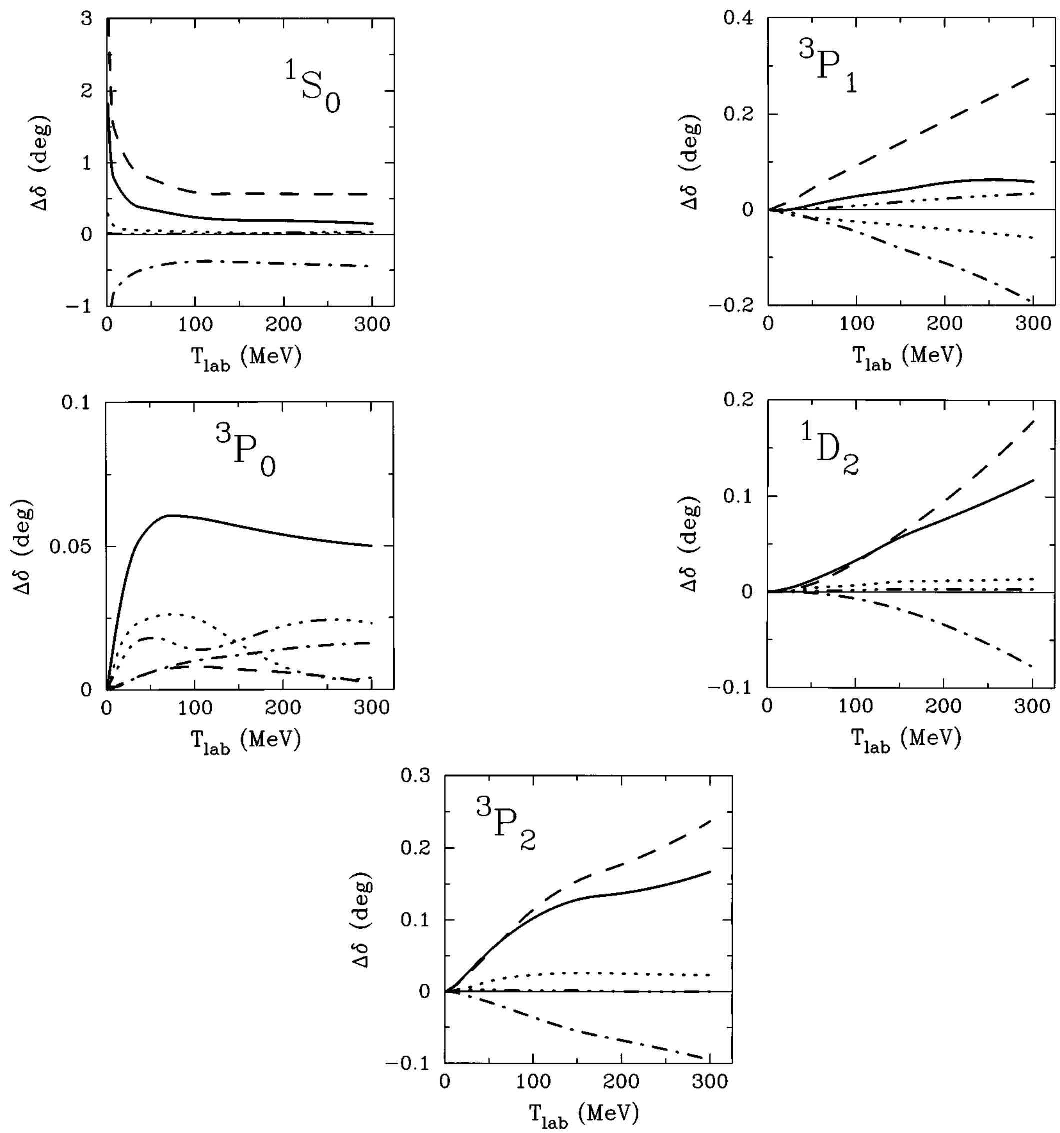

FIG. 5. CSB phase-shift differences $\Delta\delta_{\rm CSB}^{LSJ}$ (in degrees) as defined in Eq. (22) for laboratory kinetic energies $T_{\rm lab}$ below 300 MeV and partial waves with $L \leq 2$. The CSB effects due to the kinetic energy, OBE, the entire 2π model, and $\pi\rho$ exchanges are shown by the dotted, dash-triple-dotted, dashed, and dash-dotted curves, respectively. The solid curve is the sum of all CSB effects. (See text for further explanations.)

knowledge, this class of diagrams has never before been considered in any calculation of the CSB nuclear force. We find that the $\pi\rho$ diagrams give rise to non-negligible CSB contributions that are typically opposite to the 2π effects. In most partial waves, the $\pi\rho$ effect reduces the CSB from 2π exchange of the order of 50%.

Coon and Niskanen [23] have investigated the CSB effect on the singlet scattering length from the diagrams of Figs. 2 and 3, using a nonrelativistic model. Their total result $\Delta a_{\rm CSB} = 1.56$ fm (applying the de Tourreil–Rouben–Sprung NN potential [24] and a cutoff mass of 1 GeV at the pion vertices) agrees well with our total. However, there are large differences in the details: from $2\pi NN$ and $2\pi N\Delta$, Coon and Niskanen obtain 1.28 fm and 0.24 fm, respectively, while we get 0.37 fm and 1.85 fm, respectively. Thus, the ratio of the two contributions is very different. From Ref. [7] it is known that the $2\pi N\Delta$ contribution to the nuclear force is about 4 times the one from $2\pi NN$. It is reasonable to expect that the CSB effect scales roughly with the size of the contribution that generates it. This is true for our result, which is why we have confidence in our findings. In the Bonn model, a cutoff mass of 1.2 GeV is used at the pion vertices, while Coon and Niskanen use 1 GeV. This may explain why our overall contribution from 2π exchange is larger. On the other hand, our model also includes the important $\pi\rho$ diagrams (which are omitted in Ref. [23]), which reduce the overall CSB effect.

It is interesting to note that the $\Delta a_{\rm CSB} = 0.37$ fm which we get from $2\pi NN$ compares well with the $\Delta a_{\rm CSB} = 0.30$ fm obtained by Coon and Scadron [25] using the Partovi-Lomon model [26] which is a model for 2π exchange that takes only nucleons into account in intermediate states.

From the diagrams displayed in Figs. 3 and 4 it is evident that additional CSB could be created from Δ-mass splitting. Unfortunately, the charge splitting of the $\Delta(1232)$-baryon mass is not well known [9]. Since our present investigation is restricted to reliably known baryon-mass splitting, we do not consider any Δ-mass splitting and use the average value for

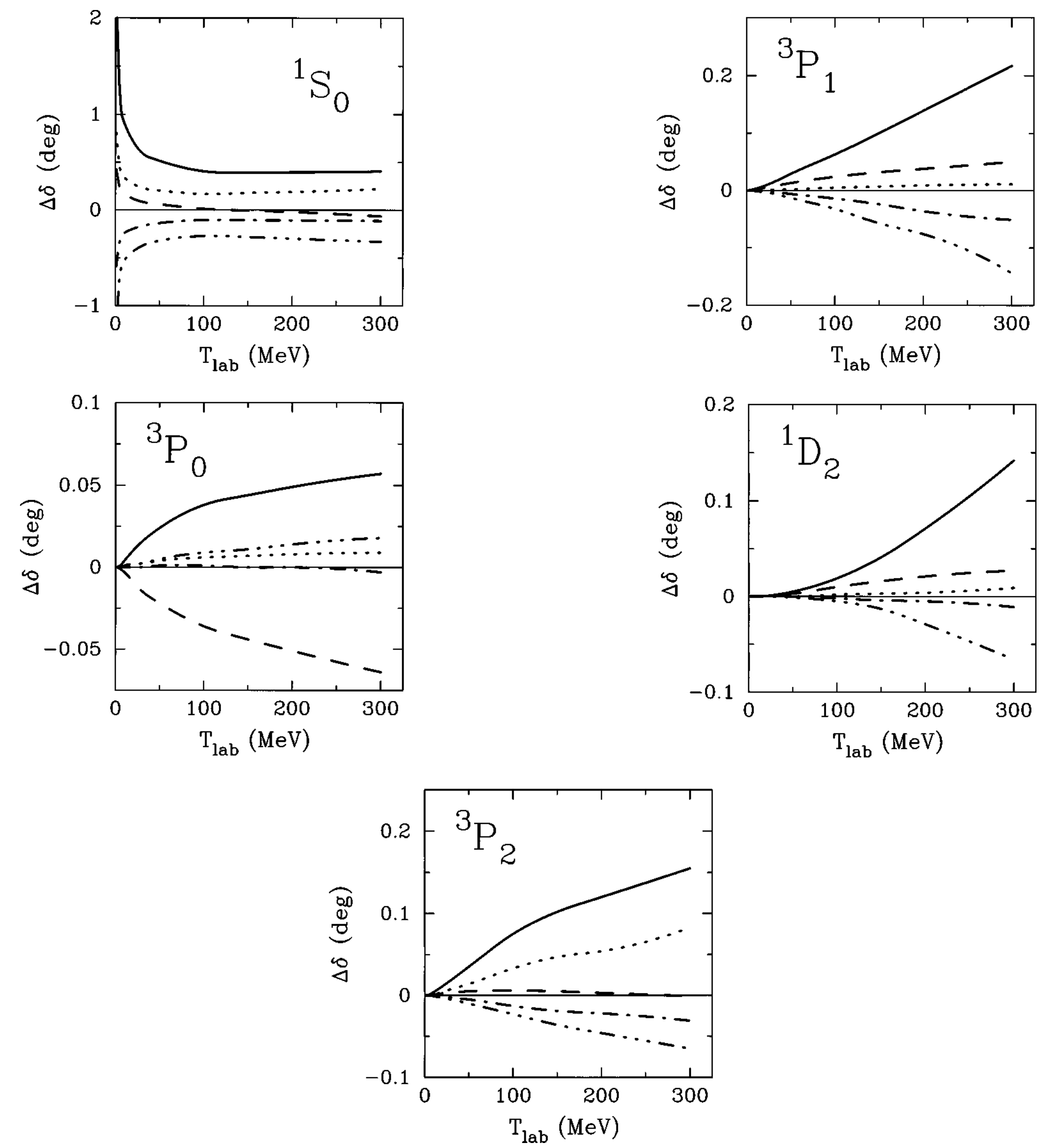

FIG. 6. Similar to Fig. 5, but here the individual contributions from the 2π and $\pi\rho$ exchange are shown. The CSB effects due to the $2\pi NN$, $2\pi N\Delta$, $2\pi\Delta\Delta$, $\pi\rho NN$, and $(\pi\rho N\Delta + \pi\rho\Delta\Delta)$ diagrams are shown by the dashed, solid, dotted, dash-dotted, and dash-triple-dotted curves, respectively. (See text for further explanations.)

the Δ mass (1232 MeV) throughout. It is, however, worthwhile to mention that our model includes everything needed for a systematic investigation of CSB effects caused by an assumed Δ-mass splitting. This may be an interesting topic for a future study.

In recent years, nuclear physicists have become increasingly concerned with chiral symmetry which is an approximate symmetry of QCD in the light-quark sector. In the light of these new views, the *NN* interaction should have a clear relationship with chiral symmetry. The Bonn model that our investigation in based upon is, by construction, not a consistently chiral model. Chiral models for the *NN* interaction and, in particular, chiral models for the 2π exchange have recently been constructed by various groups [27–29]. However, most of these models are applicable only for the peripheral partial waves of *NN* scattering and not for *S* waves, and if there are predictions for *S* waves, they are only of qualitative nature. The CSB effect in the singlet scattering length is a very subtle effect and, therefore, requires a quantitative model. Thus, current chiral models for the 2π exchange are not (yet) suitable for reliable calculations of CSB. One may then raise an interesting question: What has to be changed in the Bonn model to make it chiral? This question can be answered precisely. The diagrams in Figs. 2(a) and 2(b) of Ref. [27] have to be added to the Bonn model; that is essentially all. These diagrams include the Weinberg-Tomozawa $\pi\pi NN$ vertex which is a crucial ingredient of any nonlinear realization of chiral symmetry. However, it has been found independently by different groups [27–29] that the 2π-exchange diagrams which include the Weinberg-Tomozawa vertex make a very small, essentially negligible, contribution to the *NN* interaction. One may then expect that the CSB caused by these diagrams is also very small [30]. Thus, there are reasons to believe that the results of this study may be of broader relevance than what the (formally) nonchiral character of our model suggests. Of course, the final and reliable answer of the question under consideration can only come from a ''perfect'' and quantitative chiral model for the NN interaction that is applicable in S waves and for the calculation of scattering lengths. In view of the problems raised concerning scattering length calculations with chiral models [31,32] and in view of the continuing general controversy concerning cutoff versus dimensional regularization, it will take many years until a reliable calculation of this kind can be done. Thus, for the time being, it may be comforting to have at least our present results.

Traditionally, it was believed that ρ^0-ω mixing explains essentially all CSB in the nuclear force. However, recently some doubt has been cast on this paradigm. Some researchers [33–35] found that ρ^0-ω exchange may have a substantial q^2 dependence such as to cause this contribution to nearly vanish in NN. Our finding that the empirically known CSB in the nuclear force can be explained solely from nucleon mass splitting (leaving essentially no room for additional CSB contributions from ρ^0-ω mixing or other sources) fits well into this new scenario. However, since the issue of the q^2 dependence of ρ^0-ω exchange and its impact on NN is by no means settled (see Refs. [3,36] for critical discussions and more references), it is premature to draw any definite conclusions.

This work was supported in part by the U.S. National Science Foundation under Grant No. PHY-9603097 and by the Idaho State Board of Education.

[1] I. Slaus, Y. Akaishi, and H. Tamaka, Phys. Rep. **173**, 257 (1989).
[2] G. A. Miller, B. M. K. Nefkens, and I. Slaus, Phys. Rep. **194**, 1 (1990).
[3] G. A. Miller and W. H. T. van Oers, in *Symmetries and Fundamental Interactions in Nuclei*, edited by W. C. Haxton and E. M. Henley (World Scientific, Singapore, 1995), p. 127.
[4] R. Machleidt, Adv. Nucl. Phys. **19**, 189 (1989).
[5] R. A. Brandenburg, S. A. Coon, and P. U. Sauer, Nucl. Phys. **A294**, 305 (1978).
[6] R. A. Brandenburg, G. S. Chulick, Y. E. Kim, D. J. Klepacki, R. Machleidt, A. Picklesimer, and R. M. Thaler, Phys. Rev. C **37**, 781 (1988).
[7] R. Machleidt, K. Holinde, and Ch. Elster, Phys. Rep. **149**, 1 (1987).
[8] R. Machleidt and G. Q. Li, Phys. Rep. **242**, 5 (1994).
[9] Particle Data Group, K. Hikasa *et al.*, Phys. Rev. D **45**, S1 (1992).
[10] O. Dumbrajs *et al.*, Nucl. Phys. **B216**, 277 (1983).
[11] T. E. O. Ericson and G. A. Miller, Phys. Lett. **132B**, 32 (1983).
[12] C. Y. Cheung and R. Machleidt, Phys. Rev. C **34**, 1181 (1986).
[13] E. M. Henley, in *Isospin in Nuclear Physics*, edited by D. H. Wilkinson (North-Holland, Amsterdam, 1969), p. 16.
[14] V. Stoks, R. Timmermans, and J. J. de Swart, Phys. Rev. C **47**, 512 (1993).
[15] T. E. O. Ericson *et al.*, Phys. Rev. Lett. **75**, 1046 (1995); J. Rahm *et al.*, Phys. Rev. C **57**, 1077 (1998).
[16] R. A. Arndt, R. L. Workman, and M. M. Pavan, Phys. Rev. C **49**, 2729 (1994); R. A. Arndt, I. I. Strakovsky, and R. L. Workman, *ibid.* **52**, 2246 (1995).
[17] D. V. Bugg and R. Machleidt, Phys. Rev. C **52**, 1203 (1995).
[18] Note that in the Bonn model [7] $f_{\pi N\Delta}$ depends on $f_{\pi NN}$ via the SU(3)-based relationship
$$f^2_{\pi N\Delta}=\tfrac{72}{25}f^2_{\pi NN}.$$
[19] R. Machleidt, F. Sammarruca, and Y. Song, Phys. Rev. C **53**, 1483 (1996).
[20] R. B. Wiringa, V. G. J. Stoks, and R. Schiavilla, Phys. Rev. C **51**, 38 (1995).
[21] V. G. J. Stoks, R. A. M. Klomp, C. P. F. Terheggen, and J. J. de Swart, Phys. Rev. C **49**, 2950 (1994).
[22] H. Witala and W. Glöckle, Nucl. Phys. **A528**, 48 (1991); W. Glöckle, H. Witala, D. Hüber, H. Kamada, and J. Golak, Phys. Rep. **274**, 107 (1996); D. Hueber and J. L. Friar, ''The A_y Puzzle and the Nuclear Force,'' nucl-th/9803038.
[23] S. A. Coon and J. A. Niskanen, Phys. Rev. C **53**, 1154 (1996).
[24] R. de Tourreil, B. Rouben, and D. W. L. Sprung, Nucl. Phys. **A242**, 445 (1975).
[25] S. A. Coon and M. D. Scadron, Phys. Rev. C **26**, 2402 (1982).
[26] M. H. Partovi and E. L. Lomon, Phys. Rev. D **2**, 1999 (1970).
[27] C. Ordonez, L. Ray, and U. van Kolck, Phys. Rev. C **53**, 2086 (1996).
[28] M. R. Robilotta and C. A. da Rocha, Nucl. Phys. **A615**, 391 (1997).
[29] N. Kaiser, R. Brockmann, and W. Weise, Nucl. Phys. **A625**, 758 (1997).
[30] U. van Kolck (private communication).
[31] K. A. Scaldeferri, D. R. Philipps, C. W. Kao, and T. D. Cohen, Phys. Rev. C **56**, 679 (1997).
[32] D. B. Kaplan, M. B. Savage, and M. B. Wise, Nucl. Phys. **B478**, 629 (1996).
[33] T. Goldman, J. A. Henderson, and A. W. Thomas, Few-Body Syst. **12**, 193 (1992).
[34] J. Piekarewicz and A. G. Williams, Phys. Rev. C **47**, 2462 (1993).
[35] G. Krein, A. W. Thomas, and A. G. Williams, Phys. Lett. B **317**, 293 (1993).
[36] S. A. Coon, B. H. J. McKellar, and A. A. Rawlinson, in *Intersections between Nuclear and Particle Physics*, edited by T. W. Donelly, AIP Conf. Proc. No. 412 (AIP, Woodbury, N.Y., 1997), p. 368.